

Chromosome Segregation Errors as a Cause of DNA Damage and Structural Chromosome Aberrations

Aniek Janssen,^{1*} Marja van der Burg,² Karoly Szuhai,² Geert J. P. L. Kops,^{3†} René H. Medema^{1*†}

Various types of chromosomal aberrations, including numerical (aneuploidy) and structural (e.g., translocations, deletions), are commonly found in human tumors and are linked to tumorigenesis. Aneuploidy is a direct consequence of chromosome segregation errors in mitosis, whereas structural aberrations are caused by improperly repaired DNA breaks. Here, we demonstrate that chromosome segregation errors can also result in structural chromosome aberrations. Chromosomes that missegregate are frequently damaged during cytokinesis, triggering a DNA double-strand break response in the respective daughter cells involving ATM, Chk2, and p53. We show that these double-strand breaks can lead to unbalanced translocations in the daughter cells. Our data show that segregation errors can cause translocations and provide insights into the role of whole-chromosome instability in tumorigenesis.

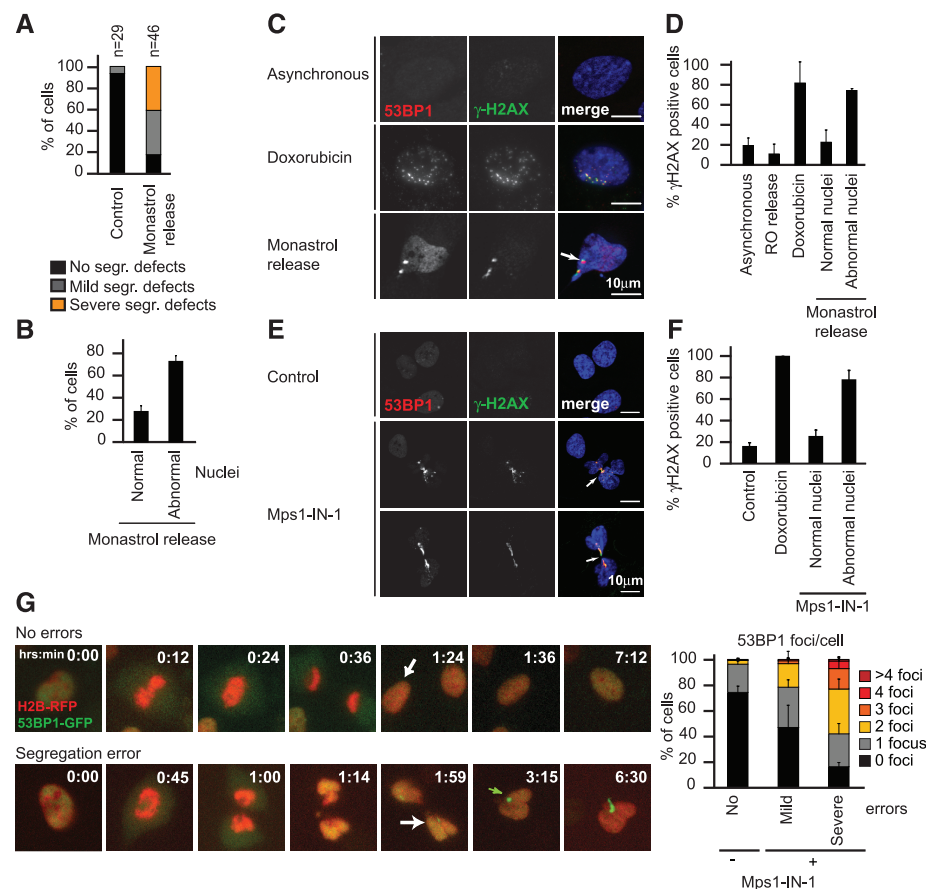
Tumor cells show two types of genetic instability: whole-chromosomal instability (CIN), in which cells frequently lose and gain whole chromosomes due to chromosome segregation errors in mitosis (1–3); and instability at the structural level of DNA, which causes small changes at the nucleotide level or larger structural aberrations at the chromosomal level, including deletions and translocations (4). These two types of genetic instability are thought to occur independently of each other (5).

To examine the impact of chromosome segregation errors on chromosome integrity, we treated hTert-immortalized, nontransformed human retinal pigment epithelial (RPE-1) cells with Monastrol to induce formation of erroneous kinetochore-microtubule attachments, in which one kinetochore is attached to both spindle poles (3, 6). Subsequent release from the Monastrol block causes a high incidence of lagging chromosomes, reflecting the situation in CIN cells (3, 7). About 80% of the RPE-1 cells blocked and released in this man-

ner improperly segregated their chromosomes, which correlated to a similar percentage of cells with abnormal nuclei (Fig. 1, A and B). Six hours after release from the Monastrol block, 70% of these abnormal nuclei displayed γ H2AX and 53BP1 foci, two markers for damaged DNA (8, 9) (Fig. 1, C and D, and fig. S1A). Conversely, only 20% of morphologically normal nuclei were positive for γ H2AX (Fig. 1D and fig. S1A). Short treatments (1 hour) with Monastrol were sufficient to induce missegregations and foci formation (fig. S1B), indicating that this does not require an extensive mitotic delay.

To exclude prolonged mitotic duration as the cause of foci formation (10–12), we provoked chromosome missegregations by inhibiting the mitotic checkpoint kinase Mps1. Cells that divided in the presence of the Mps1 inhibitor Mps1-IN-1 (13) missegregated their chromosomes

Fig. 1. (A) Quantification of chromosome missegregations after release from Monastrol block by live imaging of RPE-1 cells expressing H2B-RFP (n = number of cells). **(B)** Quantification of nuclear morphology in RPE-1 cells after release from Monastrol block (each bar represents the mean of three experiments \pm SD, 100 cells per experiment). **(C)** Images of RPE-1 acquired after indicated treatments with antibodies against 53BP1 (red) and γ H2AX (green). The DNA-damaging agent doxorubicin was used as a positive control. White arrow indicates DNA damage foci. **(D)** Quantification of γ H2AX staining in RPE-1 (each bar represents the mean of three experiments \pm SD, 100 cells per experiment). **(E)** Representative images of thymidine-synchronized cells treated without (Control) or with Mps1-IN-1 and stained as in (C). White arrow indicates DNA damage foci. **(F)** Quantification of γ H2AX staining as shown in (E), quantified as in (D). **(G)** Representative images of RPE-1 cells stably expressing H2B-RFP (red) and 53BP1-GFP (green) undergoing division in the absence or presence of missegregating chromosomes. Graph depicts quantification of 53BP1 foci formation after mitotic exit (each bar represents the mean of three experiments \pm SEM, >50 cells per experiment). White arrow depicts daughter cell that is shown in subsequent movie stills. Green arrow depicts 53BP1 foci appearance.



¹Department of Medical Oncology and Cancer Genomics Center, University Medical Center Utrecht, Universiteitsweg 100, 3584 CG, Utrecht, Netherlands. ²Department of Molecular Cell Biology, Leiden University Medical Center, Einthovenweg 20, 2300RC Leiden, Netherlands. ³Department of Molecular Cancer Research and Cancer Genomics Center, University Medical Center Utrecht, Universiteitsweg 100, 3584 CG, Utrecht, Netherlands.

*Present address: Division of Cell Biology, Netherlands Cancer Institute, Plesmanlaan 121, 1066 CX, Amsterdam, Netherlands. †To whom correspondence should be addressed. E-mail: rh.medema@nki.nl (R.H.M.); g.j.p.l.kops@umcutrecht.nl (G.J.P.L.K.)

and produced daughter cells with abnormal nuclei (Fig. 1E). Of these, 78% were γ H2AX-positive, compared to 25% in control nuclei (Fig. 1, E and F). Similar results were obtained with BJ-Tert fibroblasts (fig. S1C). Taken together, these results show that an increased frequency of chromosome missegregations is associated with the occurrence of DNA damage foci.

We next monitored chromosome segregation and appearance of DNA damage foci simultaneously in real time in RPE-1 cells stably expressing both H2B-RFP (red fluorescent protein) and 53BP1-GFP (green fluorescent protein) (Fig. 1G and movies S1 and S2). Control RPE-1 cells showed no chromosome segregation errors and, on average, only one 53BP1 focus emerged per four daughter cells (Fig. 1G). The number of cells with 53BP1 foci and the number of foci per cell increased in proportion to the severity of Mps1-IN-1-induced segregation errors (Fig. 1G). About 80% of the cells accumulated 53BP1 foci within 2 hours after a missegregation event (fig. S1D). Mps1-IN-1 also induced increased 53BP1 foci formation in U2OS human osteosarcoma cells stably expressing 53BP1-GFP (fig. S1E).

H2AX phosphorylation and 53BP1 recruitment following a segregation error were often restricted to DNA positioned in or close to the cleavage furrow (Fig. 1, E and G), suggesting

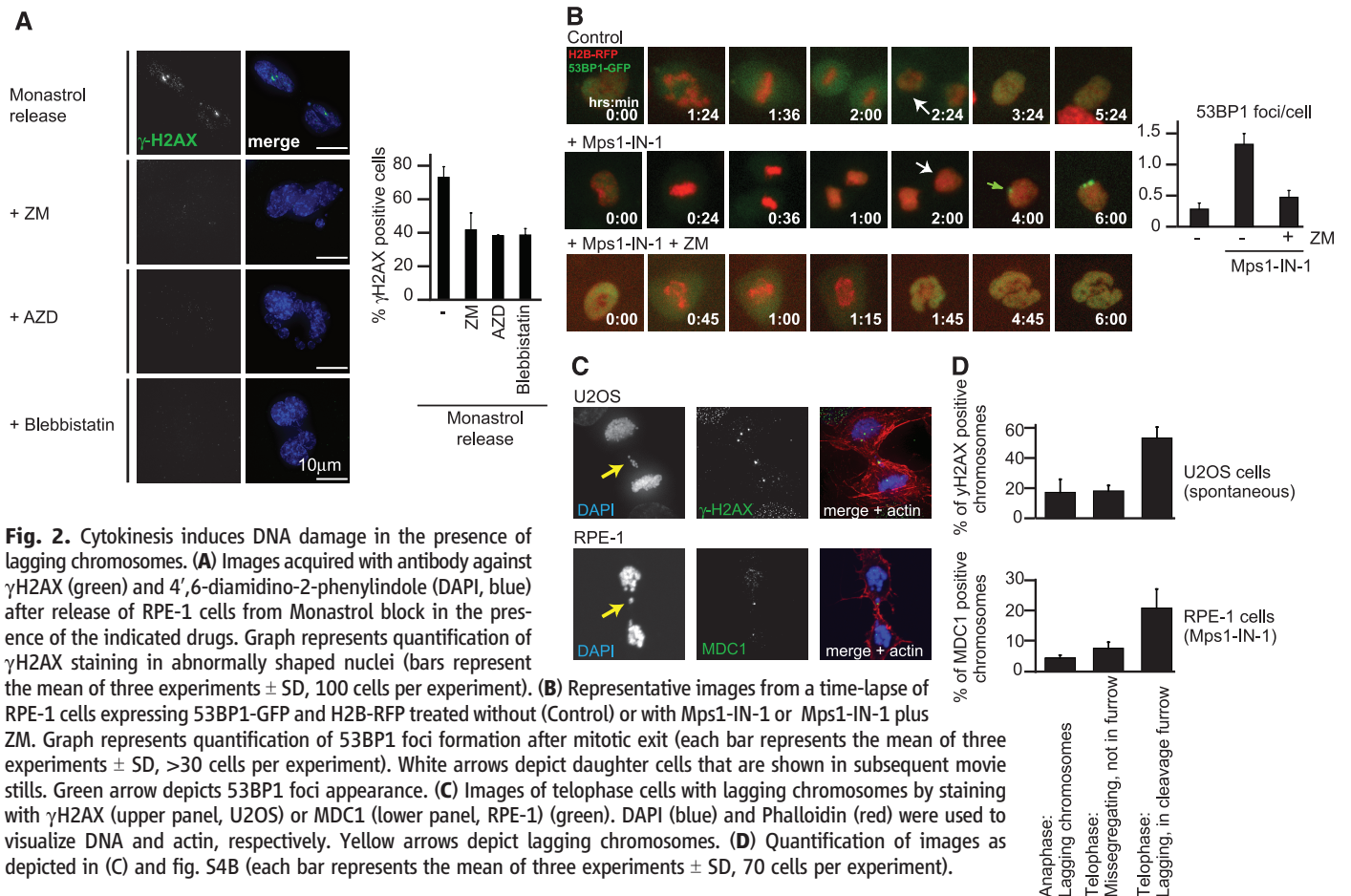
that damage might occur as a consequence of cytokinesis. We therefore prevented cytokinesis by inhibiting myosin II activity with blebbistatin (14) or by inhibiting Aurora B kinase activity with AZD1152 or ZM447439 (15, 16). Treatment of RPE-1 cells with any of these inhibitors decreased Monastrol-induced formation of γ H2AX foci in fixed cells (Fig. 2A and fig. S2A) (6) and decreased 53BP1 foci formation from 2.4 to 0.7 foci per cell in live cells (fig. S2, B to D). Similarly, inhibition of cytokinesis resulted in a 2.5-fold decrease in Mps1-IN-1-induced 53BP1 foci formation (Fig. 2B).

Chromosome missegregations as a cause of DNA damage were also apparent after spontaneous segregation errors in the CIN tumor cell lines MCF7 and SW480 (3). Chromosome missegregation events in these cells also produced enhanced 53BP1 foci formation (from an average of 0.3 to 1 or 0.7 to 1.5 foci per MCF7 or SW480 daughter cell, respectively) (fig. S3, A to C), which was again suppressed by blocking cytokinesis (fig. S3, B and C). In line with these results, U2OS cells, which display a high incidence of spontaneous segregation errors (17), have high levels of endogenous 53BP1 foci formation (average 1.2 foci per daughter cell) (fig. S1E).

These data suggest that missegregating chromosomes become damaged during cytokinesis by

cleavage furrow-generated forces. Indeed, “trapped” chromosomes positioned exactly at the site of furrow ingression (fig. S4A) stained positive for the DNA-damage markers γ H2AX and MDC1 in U2OS cells, undergoing spontaneous segregation errors, as well as in Mps1-IN-1-treated RPE-1 cells (Fig. 2, C and D, and movie S3). In comparison, foci were rarely found on missegregating chromosomes before furrow ingression or outside the cleavage furrow (fig. S4B and fig. 2D). In line with previously published data (18, 19), we found that MDC1 and γ H2AX could be recruited to DNA damage sites on mitotic chromosomes, whereas 53BP1 localization was delayed until after mitosis (Fig. 2B and fig. S1D).

If daughter cells inherit parts of broken chromosomes, the observed foci should reflect double-stranded DNA breaks (DSBs). Indeed, Monastrol-induced chromosome missegregations resulted in autophosphorylation of ataxia telangiectasia mutated (ATM) on serine 1981 (S1981) (Fig. 3A and fig. S5A), a hallmark of DSBs (20). Activated ATM is known to phosphorylate Chk2 on threonine 68 (T68) (21). Consistently, we found increased T68-phosphorylated Chk2 in cells released from a Monastrol block, which was reduced to background levels by inhibiting furrow ingression during the release (Fig. 3, C and D). pS1981-ATM and pT68-Chk2, as well as the



amount of γ H2AX-positive nuclei, were all diminished by the ATM inhibitors KU55933 (22) and caffeine (Fig. 3, A to C). Moreover, inhibition of ATM reduced 53BP1 foci formation observed during time-lapse analysis of Mps1-IN-1-treated RPE-1 cells (average of 1.3 to 0.2 foci per cell) or cells released from Monastrol block (average of 2.4 to 0.2 foci per cell) (Fig. 3, E and F, fig. S2E,

and movie S4). The observed DNA damage response therefore reflects a bona fide DSB response triggered by breakage of missegregating chromosomes during cytokinesis.

Chromosome missegregation events can activate p53 and block cell proliferation (23, 24). To assess whether cytokinesis-induced DNA damage on missegregating chromosomes can also

trigger p53 activation, we determined the effects on ATM-dependent p53 phosphorylation on serine 15 (S15) (fig. S5, B to D). Segregation errors caused an increase in the number of daughter nuclei with S15-phosphorylated p53 foci colocalizing with γ H2AX (fig. S5, C and D), which depended on cytokinesis and ATM activity (fig. S5D). Together, these data demonstrate that DSBs

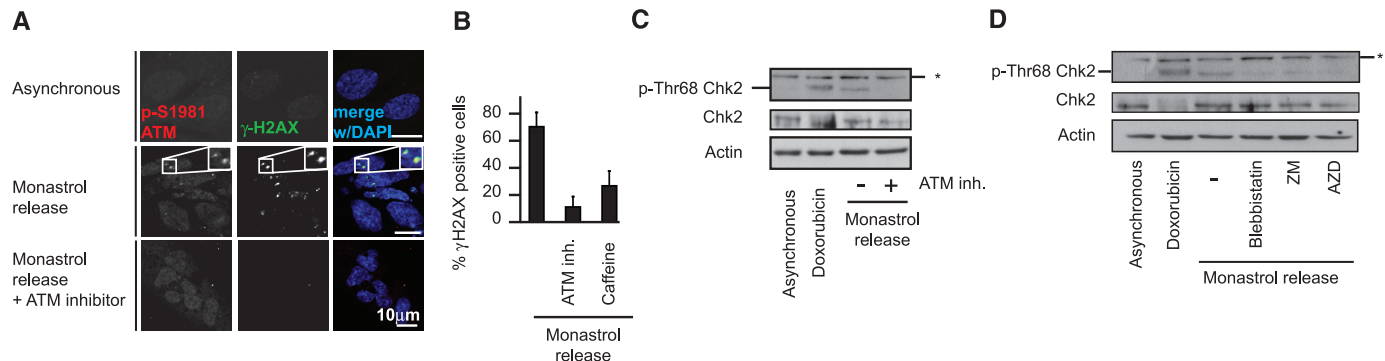
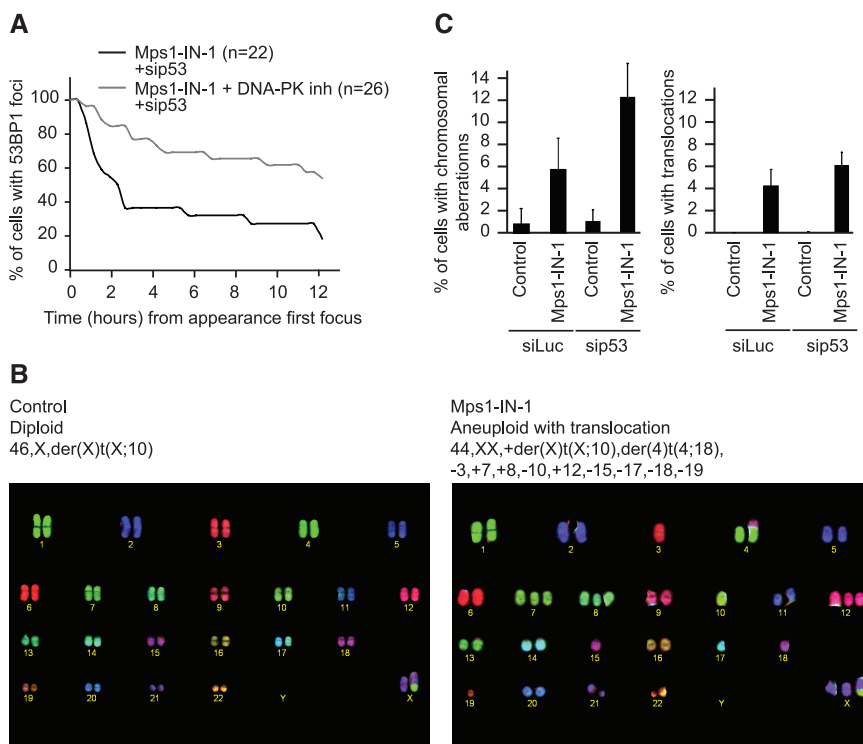


Fig. 3. Missegating chromosomes activate ATM/Chk2. (A) Images acquired with antibodies against phospho-Serine1981-ATM (red) and γ H2AX (green) after the indicated treatments. (B) Quantification of γ H2AX staining after the indicated drug treatments (abnormal nuclei only) (each bar represents the mean of three experiments \pm SD, 100 cells per experiment). (C and D) RPE-1 lysates immunoblotted for phospho-threonine-68-Chk2, total Chk2, and actin after the indicated treatments. Asterisk indicates an aspecific band. (E and F) Quantification of 53BP1-foci formation with RPE-1 live imaging after the indicated treatments (each bar represents the mean of three experiments \pm SD, 30 cells per experiment).

Fig. 4. Chromosome missegregations cause structural chromosomal aberrations. (A) Time-lapse analysis of 53BP1-foci disappearance in RPE-1 cells treated with Mps1-IN-1 with or without DNA-PK inhibitor (n = number of cells). (B) Representative images of chromosome spreads labeled with combined binary ratio labeling—fluorescence in situ hybridization 2 days after the indicated treatments. (C) Quantification of all structural aberrations (left) or chromosomal translocations only (right) after the indicated treatments (each bar represents the mean of four experiments \pm SD, 50 cells per experiment).



produced by segregation errors can activate canonical DNA damage checkpoint responses involving ATM/Chk2 and p53.

We found that ~70% of 53BP1 foci produced after segregation errors disappeared within 8 hours (Fig. 4A), suggesting that the chromosome fragments were somehow joined together, or fused to intact chromosomes. Inhibition of nonhomologous end joining (NHEJ) by inhibition or knockdown of DNA-dependent protein kinase (DNA-PK) (25) blocked mitotic entry, but this could be overcome by p53 depletion. NHEJ inhibition did not affect the appearance of 53BP1 foci in Mps1-IN-1-treated RPE-1 cells depleted of p53, but it strongly suppressed resolution of those foci (Fig. 4A and fig. S6, A to C). p53 depletion did not change the kinetics of 53BP1 foci resolution (fig. S6D). This indicated that cytokinesis-induced DNA damage is at least in part repaired via NHEJ, possibly resulting in chromosomal translocations.

Because chromosome missegregations caused DSBs that likely resulted in distribution of chromosome fragments between daughter cells, we next sought to assess whether this could cause chromosomal translocations. To this end, we examined chromosome morphology of Mps1-IN-1-treated cells (Fig. 4B) (26). As expected, inhibition of Mps1 induced overt numerical aberrations in almost all daughter cells as a consequence of whole-chromosome missegregations (13) (fig. S7A). We also observed an increased occurrence of structural chromosomal aberrations in Mps1-IN-1-treated RPE-1 cells (6%) versus control cells (0.8%) (Fig. 4, B and C, and fig. S7, B and C) (6). These structural aberrations included both broken chromosomes (fig. S7C) and unbalanced chromosomal translocations, which were observed in ~4% of Mps1-IN-1-treated RPE-1 cells, but not in control cells (Fig. 4, B and C, and fig. S7B).

Consistent with previous results (23), we found that chromosome missegregations promote a p53-dependent arrest of cells in G₁ phase (fig. S8, A and B), suggesting that p53 can suppress chromosome translocations induced by Mps1-IN-1. Indeed, depletion of p53 enhanced the occurrence of chromosomal aberrations (12% versus 6% in siLuciferase-treated cells) and unbalanced translocations (6% versus 4% in siLuciferase-treated cells) (Fig. 4C and fig. S8C). Although 70 to 80% of Mps1-IN-1-treated RPE-1 cells obtained DSBs (Fig. 1, F and G), only 6 to 12% eventually contain structural chromosomal aberrations (Fig. 4C). This indicates that most daughter cells either died or obtained both fragments of the damaged chromosome and could efficiently repair the DSBs (fig. S9).

Together, our data show that chromosomal breaks induced by segregation errors in a dividing cell can produce structural chromosomal aberrations in the daughter cells. This establishes a link between chromosome missegregations, frequently occurring in CIN cells (1, 3), and structural chromosomal aberrations, including chromosomal translocations. In line with

this, SW480-, MCF7-, and U2OS-CIN cell lines harbor many structural aberrations (fig. S10). Cytokinesis-induced DSBs can cause the separate parts of the broken chromosomes to end up in distinct daughter cells, providing a platform for an unbalanced translocation event (fig. S9). Therefore, our data imply that CIN can increase the cells' tumorigenic capacity by increasing the number of structural chromosomal aberrations in addition to changing the number of whole chromosomes.

References and Notes

1. C. Lengauer, K. W. Kinzler, B. Vogelstein, *Nature* **386**, 623 (1997).
2. R. M. Ricke, J. H. van Ree, J. M. van Deursen, *Trends Genet.* **24**, 457 (2008).
3. S. L. Thompson, D. A. Compton, *J. Cell Biol.* **180**, 665 (2008).
4. G. Obe, M. Durante, *Cytogenet. Genome Res.* **128**, 8 (2010).
5. S. L. Thompson, D. A. Compton, *Chromosome Res.* **19**, 433 (2010).
6. Materials and methods are available as supporting material on Science Online.
7. D. Cimini, *Biochim. Biophys. Acta* **1786**, 32 (2008).
8. L. B. Schultz, N. H. Chehab, A. Malikzay, T. D. Halazonetis, *J. Cell Biol.* **151**, 1381 (2000).
9. E. P. Rogakou, D. R. Pilch, A. H. Orr, V. S. Ivanova, W. M. Bonner, *J. Biol. Chem.* **273**, 5858 (1998).
10. W. B. Dalton, B. Yu, V. W. Yang, *Oncogene* **29**, 1929 (2010).
11. W. B. Dalton, M. O. Nandan, R. T. Moore, V. W. Yang, *Cancer Res.* **67**, 11487 (2007).
12. F. Quignon *et al.*, *Oncogene* **26**, 165 (2007).
13. N. Kwiatkowski *et al.*, *Nat. Chem. Biol.* **6**, 359 (2010).
14. A. F. Straight *et al.*, *Science* **299**, 1743 (2003).

15. A. A. Mortlock *et al.*, *J. Med. Chem.* **50**, 2213 (2007).
16. C. Ditchfield *et al.*, *J. Cell Biol.* **161**, 267 (2003).
17. A. Janssen, G. J. Kops, R. H. Medema, *Proc. Natl. Acad. Sci. U.S.A.* **106**, 19108 (2009).
18. S. Giunta, R. Belotserkovskaya, S. P. Jackson, *J. Cell Biol.* **190**, 197 (2010).
19. M. A. van Vugt *et al.*, *PLoS Biol.* **8**, e1000287 (2010).
20. J. H. Petrini, T. H. Stracker, *Trends Cell Biol.* **13**, 458 (2003).
21. S. Matsuoka *et al.*, *Proc. Natl. Acad. Sci. U.S.A.* **97**, 10389 (2000).
22. I. Hickson *et al.*, *Cancer Res.* **64**, 9152 (2004).
23. S. L. Thompson, D. A. Compton, *J. Cell Biol.* **188**, 369 (2010).
24. M. Li *et al.*, *Proc. Natl. Acad. Sci. U.S.A.* **107**, 14188 (2010).
25. G. C. Smith, S. P. Jackson, *Genes Dev.* **13**, 916 (1999).
26. K. Suzhai, H. J. Tanke, *Nat. Protoc.* **1**, 264 (2006).

Acknowledgments: We thank L. Kleij for technical assistance and the Medema, Lens, and Kops laboratories for discussions. We thank J. Raaijmakers, M. Tanenbaum, A. Maia, and S. Suijkerbuijk for critically reading the manuscript. We are grateful to M. van Vugt and R. Beijersbergen for sharing plasmids and cell lines. This work was supported by the Netherlands Organisation for Scientific Research (NWO) (R.H.M. and A.J.: ZonMw 918.46.616; G.J.P.L.K.: VIDI-91776336), TI Pharma (R.H.M. and A.J.: T3-105) and the European Research Council (G.J.P.L.K.: ERC-StG KINSIGN). R.H.M. was additionally funded by the Netherlands Genomic Initiative of NWO.

Supporting Online Material

www.sciencemag.org/cgi/content/full/333/6051/1895/DC1
Materials and Methods

SOM Text

Figs. S1 to S10

References (27–29)

Movies S1 to S4

23 June 2011; accepted 16 August 2011

10.1126/science.1210214

GRK2-Dependent S1PR1 Desensitization Is Required for Lymphocytes to Overcome Their Attraction to Blood

Tal I. Arnon,¹ Ying Xu,¹ Charles Lo,¹ Trung Pham,¹ Jinping An,¹ Shaun Coughlin,² Gerald W. Dorn,³ Jason G. Cyster^{1*}

Lymphocytes egress from lymphoid organs in response to sphingosine-1-phosphate (S1P); minutes later they migrate from blood into tissue against the S1P gradient. The mechanisms facilitating cell movement against the gradient have not been defined. Here, we show that heterotrimeric guanine nucleotide-binding protein-coupled receptor kinase-2 (GRK2) functions in down-regulation of S1P receptor-1 (S1PR1) on blood-exposed lymphocytes. T and B cell movement from blood into lymph nodes is reduced in the absence of GRK2 but is restored in S1P-deficient mice. In the spleen, B cell movement between the blood-rich marginal zone and follicles is disrupted by GRK2 deficiency and by mutation of an S1PR1 desensitization motif. Moreover, delivery of systemic antigen into follicles is impaired. Thus, GRK2-dependent S1PR1 desensitization allows lymphocytes to escape circulatory fluids and migrate into lymphoid tissues.

Blood and lymph contain high nM amounts of sphingosine-1-phosphate (S1P), and lymphocyte egress from lymphoid tissues is dependent on S1P triggering of S1P receptor-1 (S1PR1) on the lymphocyte (1). Within minutes of

arriving in blood, lymphocytes are able to leave again (2). In lymph nodes (LNs), this occurs via high endothelial venules (HEVs) (3, 4). Localized chemokine-mediated G_i [the family of heterotrimeric guanine nucleotide-binding protein (G protein)

Chromosome Segregation Errors as a Cause of DNA Damage and Structural Chromosome Aberrations

Aniek Janssen, Marja van der Burg, Karoly Szuhai, Geert J. P. L. Kops and René H. Medema

Science **333** (6051), 1895-1898.
DOI: 10.1126/science.1210214

ARTICLE TOOLS

<http://science.sciencemag.org/content/333/6051/1895>

SUPPLEMENTARY MATERIALS

<http://science.sciencemag.org/content/suppl/2011/09/29/333.6051.1895.DC1>

RELATED CONTENT

<http://science.sciencemag.org/content/sci/333/6051/1799.4.full>

REFERENCES

This article cites 27 articles, 14 of which you can access for free
<http://science.sciencemag.org/content/333/6051/1895#BIBL>

PERMISSIONS

<http://www.sciencemag.org/help/reprints-and-permissions>

Use of this article is subject to the [Terms of Service](#)